



Fermi National Accelerator Laboratory

FN-500
[SSC-194]
{SLAC-PUB-4783rev}

**Reactive Impedance of a
Smooth Toroidal Chamber below the
Resonance Region***

King-Yuen Ng[†]

Superconducting Super Collider Central Design Group[‡]
c/o Lawrence Berkeley Laboratory
Berkeley, California 94720

and

Robert Warnock

Stanford Linear Accelerator Center
Stanford University
Stanford, California 94309

April 1989

* Submitted to Phys. Rev. D.



SLAC-PUB-4783rev
SSC-194
FN-500
April 1989
(A)

REACTIVE IMPEDANCE OF A SMOOTH TOROIDAL CHAMBER BELOW THE RESONANCE REGION*

KING-YUEN NG[†]

*Superconducting Super Collider Central Design Group[‡]
c/o Lawrence Berkeley Laboratory, Berkeley, CA 94720*

and

ROBERT WARNOCK

Stanford Linear Accelerator Center, Stanford University, Stanford, CA 94309

ABSTRACT

We evaluate the longitudinal coupling impedance of a smooth toroidal vacuum chamber in the domain of frequencies below the first synchronous resonant mode. The chamber has rectangular cross section. With infinite wall conductivity, as assumed here, the nonresonant impedance is purely reactive. It consists of a space charge term proportional to $1/\gamma^2$ and a curvature term which survives at large γ . In the entire subresonant domain, the curvature term is well-represented as a quadratic function of frequency, namely,

$$\frac{Z}{n} = iZ_0 \left(\frac{h}{\pi R} \right)^2 \left[A - 3B \left(\frac{\nu}{\pi} \right)^2 \right],$$

where h is the height of the chamber, R is the trajectory radius and $\nu = \omega h/c$. The constants A and B are of order one, being nearly equal to one if the width of the chamber is somewhat greater than its height. Thus, ImZ/n from curvature is typically a very small fraction of an ohm below the resonance domain, which begins where $\nu > (R/h)^{1/2}$. Consequences for beam stability, if any, arise from high frequency resonances which can produce values of several ohms for Z/n .

Submitted to Physical Review D

*Work supported in part by the Department of Energy, contract DE-AC03-76SF00515.

[†] On leave from Fermi National Accelerator Laboratory, Batavia, IL 60510.

[‡] Operated by the Universities Research Association, Inc., under contracts with the U.S. Department of Energy.

I. INTRODUCTION

A beam circulating in a toroidal vacuum chamber can excite high frequency resonant modes of the entire chamber that have phase velocity equal to the particle velocity. For a chamber with a rectangular cross section of width w and height h , these synchronous modes (as excited by a centered beam) are at frequencies greater than $\omega = n\omega_o$, where $n = \pi R^{3/2}/hw^{1/2}$ and $\omega_o = \beta c/R$ is the revolution frequency. For instance, with $h = w = 3$ cm and $\beta = 1$, we have $f = \omega/2\pi > 100$ GHz for $R > 12$ m, where R is the trajectory radius. Although the frequencies are typically quite high, the impedances are so large as to provoke concern about their implications for beam stability. The impedance near the resonances, including the effects of wall resistance, was treated by Ng¹ and Warnock and Morton² in recent papers. These papers include references to much earlier work.

It is to be emphasized that the frequencies of the synchronous resonant modes are not determined by the cross-sectional dimensions of the tube alone, and therefore are unrelated to the usual tube cutoff frequencies. Due to the requirement of synchronism, these frequencies depend on the trajectory radius R . Synchronism is an effect of curvature, which comes about because the phase velocity of a wave may be greater than c at the outer torus wall and less than c at the inner wall. At a single intermediate radius R , the phase velocity can equal the particle velocity.

The impedance at low frequency, well below the tube cut-off, was derived in Ref. 2. This low frequency impedance, computed without taking account of wall resistance, turned out to be very small. It was asserted in Ref. 2 that the impedance retains a small magnitude until the resonance region is reached, but a detailed argument to support the claim was not given. Meanwhile, Ruggiero³ noticed that if the technique of the low-frequency calculation were used at higher frequency, it would predict large values of the impedance, typically tens of ohms at a few gigahertz. This observation was discussed at a workshop on the Relativistic Heavy Ion Collider, at Brookhaven National Laboratory, March 1988. According to the workshop report of Zisman,⁴ doubts about the prediction of a large impedance were raised. It was recognized that the method of calculation being used, based on the asymptotic series for Bessel functions of large argument, might not be valid in the frequency range of interest. Indeed, it was mentioned in Ref. 2 that more powerful asymptotic expansions would be needed.

The purpose of the present paper is to settle the issue by careful validation of the method of calculation. We distinguish different regions of frequency in terms of a dimensionless frequency parameter ν , defined in terms of the circular frequency ω or wave length λ as

$$\nu = \frac{\omega h}{c} = \frac{2\pi h}{\lambda} . \quad (1.1)$$

We define three regions in terms of chamber height h and trajectory radius R :

$$\begin{aligned}
 \text{Region 1:} & \quad 0 < \nu < (h/R)^{1/2} , \\
 \text{Region 2:} & \quad (h/R)^{1/2} < \nu < (R/h)^{1/2} , \\
 \text{Region 3:} & \quad \nu > (R/h)^{1/2} .
 \end{aligned} \tag{1.2}$$

The ordinary large-argument expansions of Bessel functions are valid only in the small Region 1 which lies well below the lowest tube cutoff frequency. Recall that for a rectangular tube of width w and height h , the lowest TE cutoff is at

$$\nu = \begin{cases} \pi , & h > w , \\ \frac{\pi h}{w} , & h < w . \end{cases} \tag{1.3}$$

In Region 2, the Debye expansions for $I_n(nz)$ or $J_n(ny)$ at large order n can be used. Region 3 is the resonance region, which has already been treated using the large-order uniform expansions of Olver.² The Olver expansions could also be used in Region 2, but they are more complicated and necessary only in Region 3.

It turns out that the Debye expansions can also be used in Region 1. Even though the order n tends to zero, the argument nz of $I_n(nz)$ stays large compared to one. In this limit, the large-argument and Debye expansions reduce to the same thing. Moreover, throughout Region 1, the Debye expansion produces a better approximation with a given number of terms. Consequently, we find it best to use only the Debye expansions, thereby finding a formula for the impedance that holds in the entire subresonant domain (Region 1 plus Region 2).

The formula is fitted very accurately by the quadratic form given in the Abstract. The constants A and B have simple expressions only when the width w of the chamber is somewhat greater than the height h , and in that case $A \approx B \approx 1$. Whatever the aspect ratio w/h , the ratio A/B is roughly equal to one, so the impedance has a zero near $\nu = \pi/\sqrt{3}$. A zero is expected since ImZ must be negative just below the lowest resonance.

Our calculation is based on a formula from Ref. 2 which expresses the impedance in terms of Bessel functions. The formula—which is implicit in early work of Neil⁵—is convenient for studying the nonresonant region, since it avoids any reference to the radial eigenmodes of the structure. Alternative expressions in terms of radial eigenmodes^{1,5} are awkward to evaluate in the nonresonant case, since they entail infinite sums involving all zeros of Bessel function cross products.

The general formula to be evaluated and some preparatory steps are given in Sec. 2. In Sec. 3 the Debye expansions are applied to find second order expressions

for the particular combinations of Bessel functions that occur in our formula. In Appendix A the accuracy of the second order Debye expansions is assessed; good accuracy is found in Regions 1 and 2. In Sec. 4, an analytic reduction of the general impedance formula to a tractable form is made. Section 5 gives numerical results. The analytic formula of Sec. 4 is validated by a precise calculation using Debye expansions carried to fourth order. Appendices B and C contain analytic estimates of certain functions that arise in the analysis. Although these functions are easily evaluated numerically, the analytic estimates clarify the structure of our formula.

II. THE FORMULA TO BE EVALUATED

The vacuum chamber is a torus of rectangular cross section with dimensions as defined in Fig. 1. We neglect resistivity of the walls, since it seems likely that the resistive wall effect has the same order of magnitude as in the case of a straight beam tube. Near resonances, the wall resistance is a more important issue; it was treated in the study of resonances in Refs. 1 and 2.

We use cylindrical coordinates as shown in Fig. 1. The impedance is calculated for a beam with charge density and current modeled as follows:

$$\rho(r, \theta, z, t) = q\lambda(\theta - \omega_0 t) H(z) W(r), \quad (2.1)$$

$$(J_r, J_\theta, J_z) = (0, \beta c \rho, 0), \quad (2.2)$$

$$W(r) = \frac{\delta(r - R)}{R}, \quad H(z) = H(-z). \quad (2.3)$$

The beam profile in the z direction $H(z)$ is symmetrical about $z = 0$ and we assume that it is zero outside an interval $(-\delta h, \delta h)$. We employ the Fourier transform of $H(z)$,

$$H_p = \frac{2}{h} \sin \frac{\pi p}{2} \int_{-\delta h}^{\delta h} dz \cos \left(\frac{\pi p}{h} z \right) H(z), \quad (2.4)$$

which is nonzero only for odd p , owing to the symmetry of H . In defining the impedance, we average the longitudinal field over the beam cross section.

The simple model of the beam, as described in Eqs. (2.1)–(2.3), facilitates the calculation and is adequate for present purposes. A proper discussion of beam stability requires a more general description, as will be explained in a later publication.

We are interested in the longitudinal impedance $Z(n, \omega)$ evaluated at $\omega = n\omega_0$, which is given by

$$\frac{Z(n, n\omega_0)}{n} = \frac{4\pi i Z_0}{\beta} \frac{R}{h} \sum_{p(\text{odd}) \geq 1} \Lambda_p \left[\beta^2 \frac{S_n(\Gamma_p b, \Gamma_p R) S_n(\Gamma_p R, \Gamma_p a)}{S_n(\Gamma_p b, \Gamma_p a)} + \left(\frac{\alpha_p}{\Gamma_p} \right)^2 \frac{P_n(\Gamma_p b, \Gamma_p R) P_n(\Gamma_p R, \Gamma_p a)}{P_n(\Gamma_p b, \Gamma_p a)} \right]. \quad (2.5)$$

Here $Z_0 = (\mu_0/\epsilon_0)^{1/2} = 120\pi$ ohms is the impedance of free space, and

$$\alpha_p = \frac{\pi p}{h}, \quad \Gamma_p^2 = \alpha_p^2 - \left(\frac{\omega}{c} \right)^2, \quad (2.6)$$

$$\Lambda_p = (-1)^{\frac{p-1}{2}} \frac{h}{2} \frac{\sin \frac{\pi p \delta h}{2h}}{\frac{\pi p \delta h}{2h}} H_p. \quad (2.7)$$

The P_n and S_n are cross products of modified Bessel functions:

$$\begin{aligned} P_n(x, y) &= I_n(x) K_n(y) - K_n(x) I_n(y), \\ S_n(x, y) &= I'_n(x) K'_n(y) - K'_n(x) I'_n(y). \end{aligned} \quad (2.8)$$

For notation and information on Bessel functions we refer to the article of Olver in Abramowitz and Stegun⁶ (A.-S.). If the beam profile $H(z)$ is constant on $[-\delta h, \delta h]$ and zero elsewhere, Λ_p takes the form

$$\Lambda_p = \left[\frac{\sin \frac{\pi p \delta h}{2h}}{\frac{\pi p \delta h}{2h}} \right]^2. \quad (2.9)$$

In the region where Γ_p^2 is negative, it is useful to rewrite the p -th term of Eq. (2.5) in terms of ordinary Bessel functions. Defining

$$\begin{aligned} p_n(x, y) &= J_n(x) Y_n(y) - Y_n(x) J_n(y), \\ s_n(x, y) &= J'_n(x) Y'_n(y) - Y'_n(x) J'_n(y), \end{aligned} \quad (2.10)$$

we make the transcription through

$$\begin{aligned} P_n(\Gamma_p a, \Gamma_p b) &= -\frac{\pi}{2} p_n(\gamma_p a, \gamma_p b), \\ S_n(\Gamma_p a, \Gamma_p b) &= \frac{\pi}{2} s_n(\gamma_p a, \gamma_p b), \end{aligned} \quad (2.11)$$

with

$$\gamma_p^2 = -\Gamma_p^2. \quad (2.12)$$

The first and second terms within the square brackets of Eq. (2.5) correspond to TE and TM modes, respectively. We shall label associated quantities with superscripts (E) and (M). Contrary to usual wave guide nomenclature, TE or TM here refers to a field transverse to the symmetry axis z , not to the direction of the beam.

Each of the Bessel functions in Eq. (2.5) involves an exponential factor which can be either very large or very small in the frequency range of interest. To avoid underflow and overflow in numerical evaluations and to clarify the structure of the formula, we first rearrange Eq. (2.5) to display cancellation of large exponentials against small ones. Accordingly, we write

$$\begin{aligned} \frac{S_n(\Gamma_p b, \Gamma_p R) S_n(\Gamma_p R, \Gamma_p a)}{S_n(\Gamma_p b, \Gamma_p a)} &= I'_n(\Gamma_p R) K'_n(\Gamma_p R) \frac{[1 - R_{np}^{(E)}(b, R)][1 - R_{np}^{(E)}(R, a)]}{1 - R_{np}^{(E)}(b, a)} \\ &= I'_n(\Gamma_p R) K'_n(\Gamma_p R) [1 - \sigma_{np}^{(E)}], \end{aligned} \quad (2.13)$$

$$\begin{aligned} \frac{P_n(\Gamma_p b, \Gamma_p R) P_n(\Gamma_p R, \Gamma_p a)}{P_n(\Gamma_p b, \Gamma_p a)} &= I_n(\Gamma_p R) K_n(\Gamma_p R) \frac{[1 - R_{np}^{(M)}(b, R)][1 - R_{np}^{(M)}(R, a)]}{1 - R_{np}^{(M)}(b, a)} \\ &= I_n(\Gamma_p R) K_n(\Gamma_p R) [1 - \sigma_{np}^{(M)}], \end{aligned} \quad (2.14)$$

where, with $r_1 > r_2$,

$$R_{np}^{(E)}(r_1, r_2) = \frac{K'_n(\Gamma_p r_1) I'_n(\Gamma_p r_2)}{I'_n(\Gamma_p r_1) K'_n(\Gamma_p r_2)}, \quad (2.15)$$

$$R_{np}^{(M)}(r_1, r_2) = \frac{K_n(\Gamma_p r_1) I_n(\Gamma_p r_2)}{I_n(\Gamma_p r_1) K_n(\Gamma_p r_2)}.$$

Now the initial factors $I'_n(\Gamma_p R) K'_n(\Gamma_p R)$ and $I_n(\Gamma_p R) K_n(\Gamma_p R)$ are of order unity, owing to opposite exponential factors in I_n and K_n . Moreover, we shall find that the following approximation for the ratios (2.15) holds throughout Regions 1 and 2 if $\beta \approx 1$:

$$R_{np}^{(E)}(r_1, r_2) \approx R_{np}^{(M)}(r_1, r_2) \approx \exp\{-2\pi p(r_1 - r_2)/h\}, \quad (2.16)$$

$$a \leq r_2 \leq r_1 \leq b.$$

We shall have to evaluate corrections, but the approximation Eq. (2.16) is good enough to indicate the essential structure of our formula, typically being accurate to

a few percent. If the width $w = b - a$ of the chamber is greater than or equal to the height h , then each of the exponentials occurring in Eq. (2.16) is no bigger than $\exp\{-\pi p\} \leq \exp\{-\pi\} = 0.043$. Hence, the ratios $R_{np}^{(E,M)}$ are generally negligible compared to one for $p \geq 3$, but not quite negligible for $p = 1$. The terms $\sigma_{np}^{(E,M)}$ of Eqs. (2.13) and (2.14) are small compared to one and are given by the formula

$$\sigma_{np} = \frac{R_{np}(b, R) + R_{np}(R, a) - R_{np}(b, a) - R_{np}(b, R) R_{np}(R, a)}{1 - R_{np}(b, a)}. \quad (2.17)$$

According to Eq. (2.16), the sum of the first two terms in the numerator of Eq. (2.17) is much bigger than the remaining terms, hence

$$\sigma_{np} \approx R_{np}(b, R) + R_{np}(R, a). \quad (2.18)$$

To obtain a convenient formula for further evaluation, we substitute Eq. (2.14) in Eq. (2.5) and rearrange by adding and subtracting a term. The result is

$$\begin{aligned} \frac{Z(n, n\omega_0)}{n} &= \frac{4\pi i Z_0}{\beta} \frac{R}{h} \sum_{p(\text{odd}) \geq 1} \Lambda_p \\ &\times \left\{ \left[1 - \sigma_{np}^{(M)} \right] \left[\beta^2 I'_n(\Gamma_p R) K'_n(\Gamma_p R) + \left(\frac{\alpha_p}{\Gamma_p} \right)^2 I_n(\Gamma_p R) K_n(\Gamma_p R) \right] \right. \\ &\left. + \left[\sigma_{np}^{(M)} - \sigma_{np}^{(E)} \right] \beta^2 I'_n(\Gamma_p R) K'_n(\Gamma_p R) \right\}. \end{aligned} \quad (2.19)$$

A few remarks may be helpful as a guide to our analysis of Eq. (2.19). The main object of attention will be the first term within the curly bracket. The first factor of that term, $1 - \sigma_{np}^{(M)}$, can be thought of as being equal to one as far as qualitative behavior is concerned. The two terms of the second factor, proportional to $I'_n K'_n$ and $I_n K_n$, nearly cancel at large γ so as to produce the space charge term with factor $1/\gamma^2$. The main part of the space charge term comes from the zeroth order terms in the asymptotic expansions of $I'_n K'_n$ and $I_n K_n$. Terms of next higher order produce a curvature effect which survives at infinite γ . This curvature term is the principal object of interest. The second term within the curly brackets in Eq. (2.19) is also a curvature term (plus a small correction to the space charge term), opposite in sign to the main curvature term, but in most cases smaller in magnitude. It rapidly dwindles in importance as the aspect ratio w/h of the chamber increases ($w =$ width, $h =$ height). Thus, there is no close cancellation between the curvature effects of the two terms in Eq. (2.19), a circumstance which simplifies the assessment of higher order terms.

III. DEBYE EXPANSIONS

We are concerned with Bessel functions of order n and argument $\Gamma_p r$ with $r = a, R, b$. In terms of $\nu = \omega h/c$, we have

$$n = \frac{\nu R}{\beta h} , \quad (3.1)$$

$$\Gamma_p r = [(\pi p)^2 - \nu^2]^{1/2} \frac{r}{h} , \quad p = 1, 3, \dots , \quad (3.2)$$

For small ν , $\Gamma_p r$ is large compared to one, leading to asymptotic expansions for large argument. One must remember, however, that the success of such expansions depends on the order, as well as the argument, and that the order n increases with ν . The argument must be large compared to n^2 . Hence, the use of large-argument expansions is restricted to the small Region 1, as defined in Eq. (1.2). This is explained in Appendix A.

At the lower end of Region 2 we have $n > (R/h)^{1/2}$, which is large compared to one. We are thus led to consider the Debye expansions, which are useful at large n . Let us divide Region 2 into two parts:

$$\text{Region 2a:} \quad \left(\frac{h}{R}\right)^{1/2} < \nu < \pi p , \quad (3.3)$$

$$\text{Region 2b:} \quad \pi p < \nu < \left(\frac{R}{h}\right)^{1/2} , \quad (3.4)$$

the second part being empty at large p . In Region 2a we deal with modified Bessel functions since $\Gamma_p r > 0$. The relevant Debye expansions are as follows: (A.-S. 9.7.7-9.7.10):

$$I_n(nz) \sim \left(\frac{1}{2\pi n}\right)^{1/2} \frac{e^{n\eta}}{(1+z^2)^{1/4}} [1 + c_1 + c_2 + c_3 + \dots] , \quad (3.5)$$

$$K_n(nz) \sim \left(\frac{\pi}{2n}\right)^{1/2} \frac{e^{-n\eta}}{(1+z^2)^{1/4}} [1 - c_1 + c_2 - c_3 + \dots] , \quad (3.6)$$

$$I'_n(nz) \sim \left(\frac{1}{2\pi n}\right)^{1/2} \frac{(1+z^2)^{1/4}}{z} e^{n\eta} [1 + d_1 + d_2 + d_3 + \dots] , \quad (3.7)$$

$$K'_n(nz) \sim -\left(\frac{\pi}{2n}\right)^{1/2} \frac{(1+z^2)^{1/4}}{z} e^{-n\eta} [1 - d_1 + d_2 - d_3 + \dots] , \quad (3.8)$$

where

$$\eta(z) = (1 + z^2)^{1/2} + \ln \left[\frac{z}{1 + (1 + z^2)^{1/2}} \right], \quad (3.9)$$

$$c_1 = \frac{1}{24} (3t - 5t^3) \frac{1}{n}, \quad c_2 = \frac{1}{1152} (81t^2 - 462t^4 + 385t^6) \frac{1}{n^2}, \quad (3.10)$$

$$d_1 = \frac{1}{24} (-9t + 7t^3) \frac{1}{n}, \quad d_2 = \frac{1}{1152} (-135t^2 + 594t^4 - 455t^6) \frac{1}{n^2}, \quad (3.11)$$

$$t = \frac{1}{(1 + z^2)^{1/2}}. \quad (3.12)$$

These expansions are valid at large n , with accuracy uniform in z for large $|\arg z| \leq \pi/2 - \epsilon$, any $\epsilon > 0$.

The analytic continuation of Eqs. (3.5) and (3.8) through $z = 0$ to imaginary z , $\arg z = \pi/2$, also yields valid asymptotic expansions. These are the Debye asymptotic expansions for the ordinary Bessel functions $J_n(ny), \dots, y = \text{Im}z$. They have the following form (A.-S. 9.3.7, 9.3.8, 9.3.11, 9.3.12):

$$J_n(ny) \sim \left(\frac{1}{2\pi n} \right)^{1/2} \frac{e^{-n\xi}}{(1 - y^2)^{1/4}} [1 + c_1 + c_2 + c_3 + \dots], \quad (3.13)$$

$$Y_n(ny) \sim - \left(\frac{2}{\pi n} \right)^{1/2} \frac{e^{n\xi}}{(1 - y^2)^{1/4}} [1 - c_1 + c_2 - c_3 + \dots], \quad (3.14)$$

$$J'_n(ny) \sim \left(\frac{1}{2\pi n} \right)^{1/2} \frac{(1 - y^2)^{1/4}}{y} e^{-n\xi} [1 + d_1 + d_2 + d_3 + \dots], \quad (3.15)$$

$$Y'_n(ny) \sim - \left(\frac{2}{\pi n} \right)^{1/2} \frac{(1 - y^2)^{1/4}}{y} e^{n\xi} [1 - d_1 + d_2 - d_3 + \dots], \quad (3.16)$$

where

$$\xi(y) = -(1 - y^2)^{1/2} - \ln \left[\frac{y}{1 + (1 - y^2)^{1/2}} \right], \quad (3.17)$$

and the c_i, d_i are given by Eqs. (3.10) and (3.11) but with

$$t = \frac{1}{(1 - y^2)^{1/2}}. \quad (3.18)$$

These expansions are valid at large n , but their accuracy is not uniform in y near $y = 1$, owing to the singularity of t at $y = 1$. For a uniform approximation near $y = 1$, the Olver expansions can be used (A.-S. 9.3.35, 9.3.36, 9.3.43, 9.3.44).

The expansions (3.13)–(3.16) are valid in Region 2b, with $ny = \gamma_p r$, $\gamma_p^2 = -\Gamma_p^2$. At the upper end of Region 2b, the expansions begin to fail owing to the singularity of t at $y = 1$. The upper bound of Region 2b is determined in App. A.

Our formulas make a smooth transition from Region 2a to Region 2b, owing to analytic continuation. In the continuation from real $z = \Gamma_p r/n$ to imaginary $z = iy = i\gamma_p r/n$, we pick up $\ln(i) = i\pi/2$ in Eq. (3.9). The impedance involves η only in differences $\eta(z_1) - \eta(z_2)$, so that the $\ln(i)$ terms all cancel. If we write the impedance in terms of Eqs. (3.5)–(3.8) and redefine η to be

$$\eta(z) = (1 + z^2)^{1/2} + \ln \left[\frac{|z|}{1 + (1 + z^2)^{1/2}} \right], \quad (3.19)$$

then the formula holds in all of Region 2, with

$$z_r^2 = \left(\frac{\Gamma_p r}{n} \right)^2 = \left(\beta \frac{r}{R} \right)^2 \left[\left(\frac{\pi p}{\nu} \right)^2 - 1 \right]. \quad (3.20)$$

The particular combinations of Bessel functions that appear in the impedance Eq. (2.19) are obtained in Debye expansion as follows:

$$I_n(nz) K_n(nz) \sim \frac{1}{2n} \frac{1}{(1 + z^2)^{1/2}} [1 + 2c_2 - c_1^2 + 2c_4 - 2c_1 c_3 + c_2^2 + \dots], \quad (3.21)$$

$$I'_n(nz) K'_n(nz) \sim -\frac{1}{2n} \frac{(1 + z^2)^{1/2}}{z^2} [1 + 2d_2 - d_1^2 + 2d_4 - 2d_1 d_3 + d_2^2 + \dots], \quad (3.22)$$

$$R_{np}^{(M)}(r_1, r_2) \sim \exp \{ -2n [\eta(z_{r_1}) - \eta(z_{r_2})] \} \frac{[1 + \sum_k (-1)^k c_k(r_1)][1 + \sum_k c_k(r_2)]}{[1 + \sum_k c_k(r_1)][1 + \sum_k (-1)^k c_k(r_2)]}, \quad (3.23)$$

$$r_1 > r_2 .$$

A formula like Eq. (3.23) holds for $R_{np}^{(E)}$, but with d_k replacing c_k . Appendix A shows that one can get an excellent approximation in Region 2, and also in Region 1, by retaining just terms through second order in Eqs. (3.21)–(3.23). To second order, Eq. (3.23) involves only the coefficient c_1 :

$$R_{np}^{(M)}(r_1, r_2) \sim \exp \{ -2n [\eta(z_{r_1}) - \eta(z_{r_2})] \} \left\{ 1 + 2 [c_1(r_2) - c_1(r_1)] + 2 [c_1(r_2) - c_1(r_1)]^2 \right\}, \quad r_1 > r_2. \quad (3.24)$$

The coefficient c_2 appears first in third order.

IV. FORMULA FOR THE IMPEDANCE VALID IN REGIONS 1 AND 2

We evaluate the impedance as given by Eq. (2.19), with $\sigma_{np}^{(E,M)}$ as determined by Eq. (2.18). The functions $I_n K_n$ and $I'_n K'_n$ are computed by the series (3.21), Eq. (3.22) carried to second-order, and $R_{np}^{(M,E)}$ is given by Eq. (3.24) and the similar formula with $M \rightarrow E, c_1 \rightarrow d_1$.

We define $z_r = \Gamma_p r/n$, but write plain z for z_R since the latter occurs very often. The following relations are useful:

$$z^2 = \beta^2 \left[\left(\frac{\pi p}{\nu} \right)^2 - 1 \right], \quad (4.1)$$

$$\frac{1}{n} = \frac{1}{\pi p} \frac{h}{R} (z^2 + \beta^2)^{1/2} = \frac{\beta}{\nu} \frac{h}{R}, \quad (4.2)$$

$$\left(\frac{\alpha_p}{\Gamma_p} \right)^2 = 1 + \left(\frac{\beta}{z} \right)^2, \quad (4.3)$$

$$z_r = \frac{r}{R} z = \frac{\Gamma_p r}{n}. \quad (4.4)$$

In the following work, most expressions depend on the three variables ν, p, β . To avoid ugly notation we often suppress explicit reference to one or more of these variables.

For the second-order terms of Eqs. (3.12) and (3.22), we apply Eqs. (3.10) and (3.11) to find

$$2c_2(R) - c_1^2(R) = \frac{z^2(z^2 - 4)}{8n^2(1 + z^2)^3}, \quad (4.5)$$

$$2d_2(R) - d_1^2(R) = \frac{z^2(-3z^2 + 4)}{8n^2(1 + z^2)^3}. \quad (4.6)$$

With the definition

$$t_r = \frac{1}{(1 + z_r^2)^{1/2}}, \quad (4.7)$$

the differences that appear in $R_{np}^{(M,E)}$ are

$$c_1(b) - c_1(R) = \frac{t_b - t_R}{24n} [3 - 5(t_b^2 + t_b t_R + t_R^2)], \quad (4.8)$$

$$d_1(b) - d_1(R) = \frac{t_b - t_R}{24n} [-9 + 7(t_b^2 + t_b t_R + t_R^2)]. \quad (4.9)$$

From Eqs. (3.24) and (2.18) we have

$$\begin{aligned} \sigma_{np}^{(M)} = & \exp\{-2n[\eta(z_b) - \eta(z_R)]\} \left\{ 1 - 2[c_1(b) - c_1(R)] + 2[c_1(b) - c_1(R)]^2 \right\} \\ & + \exp\{-2n[\eta(z_R) - \eta(z_a)]\} \left\{ 1 - 2[c_1(R) - c_1(a)] + 2[c_1(R) - c_1(a)]^2 \right\}. \end{aligned} \quad (4.10)$$

The formula for $\sigma_{np}^{(E)}$ is the same, but with d_1 replacing c_1 .

Our main concern is the second factor in the first term of Eq. (2.19) which we denote by Φ . After substitution of Eqs. (3.21), (3.22), (4.3), (4.5), and (4.6), and a short computation, we find

$$\begin{aligned} \Phi = & \beta^2 I'_n(\Gamma_p R) K'_n(\Gamma_p R) + \left(\frac{\alpha_p}{\Gamma_p}\right)^2 I_n(\Gamma_p R) K_n(\Gamma_p R) \\ = & \frac{1}{2n(1+z^2)^{1/2}} \left\{ \frac{1}{\gamma^2} + \frac{1}{8n^2(1+z^2)^3} [-8\beta^2 - 4z^2 + (1+3\beta^2)z^4] \right\}. \end{aligned} \quad (4.11)$$

The derivation of Eq. (4.11) was simplified by using the variable z . To make the frequency dependence more evident, we now return to the variable ν by applying Eqs. (4.1) and (4.2). The result is

$$\begin{aligned} \Phi = & \frac{h}{2R} \frac{1}{[(\pi p)^2 + (\nu/\beta\gamma)^2]^{1/2}} \left\{ \frac{1}{\gamma^2} + \frac{1}{2} \left[\frac{h}{R}\right]^2 \frac{1}{[(\pi p)^2 + (\nu/\beta\gamma)^2]^3} \right. \\ & \left. \times \left(\frac{1+3\beta^2}{4} [(\pi p)^2 - \nu^2]^2 - \frac{\nu^2}{\beta^2} [(\pi p)^2 + \nu^2] \right) \right\} \end{aligned} \quad (4.12)$$

Since the terms involving ν^4 cancel at $\beta = 1$, it is useful to extract terms having a factor $1/\gamma^2$. Accordingly, we note that $\beta^2 = 1 - 1/\gamma^2$, $1/\beta^2 = 1 + 1/(\beta\gamma)^2$ and rearrange Eq. (4.12) to obtain

$$\Phi = \frac{h}{2\pi p R} \frac{1}{[1 + (\nu/\pi p \beta \gamma)^2]^{1/2}} \left\{ \frac{S_p(\beta, \nu)}{\gamma^2} + \frac{1}{2} \left(\frac{h}{\pi p R}\right)^2 \frac{1 - 3(\nu/\pi p)^2}{[1 + (\nu/\pi p \beta \gamma)^2]^3} \right\}, \quad (4.13)$$

where

$$\begin{aligned} S_p(\beta, \nu) = & 1 - \frac{1}{8} \left(\frac{h}{\pi p R}\right)^2 \frac{1}{[1 + (\nu/\pi p \beta \gamma)^2]^3} \\ & \times \left[3 + \left(\frac{4}{\beta^2} - 6\right) \left(\frac{\nu}{\pi p}\right)^2 + \left(3 + \frac{4}{\beta^2}\right) \left(\frac{\nu}{\pi p}\right)^4 \right]. \end{aligned} \quad (4.14)$$

The second term in Eq. (4.14) is small compared to one throughout Regions 1 and 2; for most purposes, we can put $S_p = 1$. We refer to the first term of Eq. (4.13) as the *space charge term*, and the second term as the *curvature term*.

Next we evaluate the second term in the curly brackets of Eq. (2.19). Denoting the latter by Ψ , and invoking Eq. (3.22) carried to second order, we have

$$\begin{aligned}\Psi &= \left[\sigma_{np}^{(M)} - \sigma_{np}^{(E)} \right] \beta^2 I'_n(\Gamma_p R) K'_n(\Gamma_p R) \\ &= -\frac{\beta^2}{2n} \frac{(1+z^2)^{1/2}}{z^2} \left[\sigma_{np}^{(M)} - \sigma_{np}^{(E)} \right] [1 + 2d_2 - d_1^2] ,\end{aligned}\tag{4.15}$$

where

$$\begin{aligned}\sigma_{np}^{(M)} - \sigma_{np}^{(E)} &= 2 \exp\{-2n[\eta(z_b) - \eta(z_R)]\} \tau(b, R) [1 + \epsilon(b, R)] \\ &\quad + 2 \exp\{-2n[\eta(z_R) - \eta(z_a)]\} \tau(R, a) [1 + \epsilon(R, a)] ,\end{aligned}\tag{4.16}$$

$$\tau(b, R) = -c_1(b) + c_1(R) + d_1(b) - d_1(R) = \frac{t_R - t_b}{2n} [1 - t_b^2 - t_b t_R - t_R^2] ,$$

$$\epsilon(b, R) = -c_1(b) + c_1(R) - d_1(b) + d_1(R) = \frac{t_R - t_b}{12n} [-3 + t_b^2 + t_b t_R + t_R^2] .\tag{4.17}$$

Although Ψ usually has minor importance, it requires a relatively complicated analysis, most of which we relegate to Appendices B and C. Here, we put down the leading approximation to Ψ , denoted by Ψ_o , which is entirely adequate for our purposes. The corrections are estimated in the Appendices. First, we note that the exponents in Eq. (4.16) are well-approximated as follows (throughout Regions 1 and 2):

$$2n [\eta(z_b) - \eta(z_R)] \approx 2\pi p \frac{b-R}{h} \left[1 + \left(\frac{\nu}{\gamma\beta\pi p} \right)^2 \right]^{1/2} ,\tag{4.18}$$

We derive this rather surprising result in Appendix C and obtain bounds for the error of the approximation. Thus, for a centered, relativistic beam with $\pi\gamma \gg \nu$, Eq. (4.16) entails a factor $\exp\{-\pi p w/h\}$. As a result of this factor, the importance of Ψ diminishes rapidly with increasing aspect ratio w/h . The final factor in Eq. (4.18), usually close to one, will be denoted by μ_p :

$$\mu_p(\beta, \nu) = \left[1 + \left(\frac{\nu}{\gamma\beta\pi p} \right)^2 \right]^{1/2} .\tag{4.19}$$

For the leading approximation to Ψ we use Eq. (4.18), dropping $2d_2 - d_1^2$ in Eq. (4.15) and $\epsilon(b, R), \epsilon(R, a)$ in Eq. (4.16). The dropped terms are small compared to one, as shown in Appendix B. Using Eqs. (4.1)-(4.4) and (3.12), we find that

$$\Psi \approx \Psi_o = -\frac{\beta^4}{2\nu^2} \left(\frac{h}{R}\right)^2 [A_p(b, R) + A_p(R, a)] , \quad (4.20)$$

where

$$A_p(b, R) = \exp\{-2\pi p \mu_p (b - R)/h\} \frac{t_b^2 t_R [1 - t_b^2 - t_b t_R - t_R^2]}{t_b + t_R} \frac{b^2 - R^2}{R^2} . \quad (4.21)$$

In Appendix B we estimate Ψ_o at all frequencies $\nu < (R/h)^{1/2}$. Here, we merely note that the magnitude of Ψ_o at $\nu = \pi p$ is evident, since the t_r all equal one at that point. For a centered beam with $\beta = 1$ we have

$$\Psi_o|_{\nu=\pi p} = \frac{w}{R} \left(\frac{h}{\pi p R}\right)^2 \exp\{-\pi p w/h\} ,$$

which is to be compared with Φ as given in Eq. (4.13),

$$\Phi|_{\nu=\pi p} = -\frac{1}{2} \left(\frac{h}{\pi p R}\right)^3 .$$

Thus,

$$\frac{\Psi_o}{\Phi} \Big|_{\nu=\pi p, \beta=1} = -2\pi p \frac{w}{h} \exp\{-\pi p w/h\} ,$$

so that Ψ_o is negligible compared to Φ for $p \geq 3$ and also negligible even for $p = 1$, if the aspect ratio w/h is fairly big, say $w/h \geq 2$. It happens that the same is true at all frequencies, the ratio Ψ_o/Φ always being negative.

To evaluate Eq. (2.19) we also need

$$1 - \sigma_{np}^{(M)} \approx 1 - \exp\{-2\pi p \mu_p (b - R)/h\} - \exp\{-2\pi p \mu_p (R - a)/h\} . \quad (4.22)$$

The corrections to this quantity from the other terms indicated in Eq. (4.10) are not important, since the exponential terms in Eq. (4.22) are already small compared to one.

We can now assemble the impedance Eq. (2.19) from Eqs. (4.13), (4.20) and (4.22). The result is:

$$\begin{aligned}
\frac{Z(n, n\omega_o)}{n} = & \frac{2iZ_o}{\beta} \sum_{p(\text{odd}) \geq 1} \frac{\Lambda_p}{\mu_p} \frac{1}{p} \left[1 - \exp \{-2\pi p \mu_p (b - R)/h\} - \exp \{-2\pi p \mu_p (R - a)/h\} \right] \\
& \times \left\{ \frac{S_p}{\gamma^2} + \frac{1}{2} \left(\frac{h}{\pi p R} \right)^2 \frac{1}{\mu_p^6} \left[1 - 3 \left(\frac{\nu}{\pi p} \right)^2 \right] \right\} \\
& - \frac{2\pi i Z_o \beta^3}{\nu^2} \frac{h}{R} \sum_{p(\text{odd}) \geq 1} \Lambda_p [A_p(b, R) + A_p(R, a)] .
\end{aligned} \tag{4.23}$$

Unless $(b - R)/h$ or $(R - a)/h$ is unusually small (the beam is near the wall of the chamber), the summand of the second sum in Eq. (4.23) is negligible for $p \geq 3$; the same is true of the exponential terms in the first sum. Moreover, μ_p is close to one for a relativistic beam, certainly if $\gamma^2 \gg R/(\pi^2 h)$. The factor Λ_p defined in (2.7) is equal to one for an infinitely thin beam ($\delta h \rightarrow 0$). The space charge term involving S_p/γ^2 diverges in the limit $\delta h \rightarrow 0$, but the curvature term will be finite in the limit and not differ much from its value for realistic δh . Thus, for a relativistic beam for which the space charge term is negligible and the beam is not too close to the chamber wall, we have the following good approximation:

$$\begin{aligned}
\frac{Z(n, n\omega_o)}{n} = & iZ_o \left(\frac{h}{\pi R} \right)^2 \left\{ \left[1 - \exp \{-2\pi(b - R)/h\} - \exp \{-2\pi(R - a)/h\} \right] \right. \\
& \times \left. \left[1 - 3 \left(\frac{\nu}{\pi} \right)^2 \right] + \sum_{p(\text{odd}) \geq 3} \frac{1}{p^3} \left[1 - 3 \left(\frac{\nu}{\pi p} \right)^2 \right] \right\} + \rho
\end{aligned}$$

where

$$\rho = \frac{-2\pi i Z_o}{\nu^2} \frac{h}{R} [A_1(b, R) + A_1(R, a)] . \tag{4.24}$$

The residual sums in Eq. (4.24) may be expressed in terms of the zeta function (A.-S., 23.2.20):

$$\begin{aligned}\sum_{p(\text{odd}) \geq 3} \frac{1}{p^3} &= \frac{7}{8} \zeta(3) - 1 = 0.05179, \\ \sum_{p(\text{odd}) \geq 3} \frac{1}{p^5} &= \frac{31}{32} \zeta(5) - 1 = 0.004516.\end{aligned}\tag{4.25}$$

We then have

$$\begin{aligned}\frac{Z(n, n\omega_0)}{n} &= \\ &= iZ_0 \left(\frac{h}{\pi R}\right)^2 \left\{ \left[1 - \exp\{-2\pi(b-R)/h\} - \exp\{-2\pi(R-a)/h\} \right] \right. \\ &\times \left[1 - 3 \left(\frac{\nu}{\pi}\right)^2 \right] + 0.05179 - 0.01355 \left(\frac{\nu}{\pi}\right)^2 \left. \right\} + \rho \\ &= iZ_0 \left(\frac{h}{\pi R}\right)^2 \left[A - 3B \left(\frac{\nu}{\pi}\right)^2 \right] + \rho,\end{aligned}\tag{4.26}$$

where the constants A , B are nearly equal to one. At fairly large aspect ratio of the chamber, say $w/h \geq 2$, the term ρ is negligible and we get a simple quadratic dependence on frequency.

The numerical evaluation of the following section shows that Z/n retains a nearly quadratic dependence on frequency, even when ρ is not negligible.

V. NUMERICAL EVALUATION OF IMPEDANCE

Here we show results for representative parameters, obtained from the formula (4.23) for the impedance; the simplified formula (4.26) gives practically the same results. Since certain approximations were made in the derivation of these formulas, notably in the treatment of terms with exponential factors, we first test Eq. (4.23) against a calculation in which the only approximation is the truncation of Debye asymptotic expansions at such a point as to insure high accuracy, namely at fourth order in $1/n$.

In the Debye expansion of the function Φ of Eq. (4.11), the zeroth-order terms—nearly cancelling—produce the space-charge term

$$\frac{1}{2n(1+z^2)^{1/2}} \frac{1}{\gamma^2}.\tag{5.1}$$

There are no near cancellations in the remaining terms of Φ , so we can evaluate them routinely with a computer. Invoking Eqs. (3.21) and (3.22), we obtain

$$\Phi = \frac{1}{2n(1+z^2)^{1/2}} \left[\frac{1}{\gamma^2} - \beta^2 \frac{1+z^2}{z^2} (2d_2 - d_1^2 + 2d_4 - 2d_1d_3 + d_2^2 + \dots) + \left(\frac{\alpha_p}{\Gamma_p} \right)^2 (2c_2 - c_1^2 + 2c_4 - 2c_1c_3 + c_2^2 + \dots) \right]. \quad (5.2)$$

We use Eq. (5.2), retaining terms to fourth order as indicated, and obtain R_{np} from Eq. (3.23). [We use Eq. (3.23) as it stands, truncating each of the four component series after $k = 4$, but making no further simplification]. We then compute σ_{np} from its exact definition, Eq. (2.17), thus obtaining all of the ingredients for an accurate evaluation of the impedance through Eq. (2.19). Admittedly, there is a close cancellation in the difference $\sigma_{np}^{(M)} - \sigma_{np}^{(E)}$, but in our double precision calculation the difference still has eight significant digits.

Figure 2 gives the resulting impedance for $\nu < (R/h)^{1/2}$ with the following parameters, which are nominal values for the SLC damping rings:

$$R = 5.7 \text{ m}, \quad w = h = 0.02 \text{ m}, \quad \beta = 1. \quad (5.3)$$

We take Λ_p from Eq. (2.9) with $\delta h = 1 \text{ mm}$, and include enough axial modes p so that convergence is clearly observed. The accurate curve is the solid line and the result of formula (4.23) is the dashed line. We fit a quadratic to the accurate curve, passing it through the values at $\nu = 0$ and $\nu = (R/h)^{1/2}$. The quadratic is

$$\frac{ImZ}{n} = Z_o \left(\frac{h}{\pi R} \right)^2 \left[A - 3B \left(\frac{\nu}{\pi} \right)^2 \right], \quad (5.4)$$

$$A = 0.7153, \quad B = 0.6714.$$

It fits the accurate curve to three digits at all ν . Repeating the calculation at larger and smaller aspect ratios, we again find that Eq. (5.4) holds to three digits with

$$\begin{aligned} A = 1.009 \quad , \quad B = 0.9766 \quad , \quad (w = 0.02 \text{ m} \quad , \quad h = 0.01 \text{ m}) \quad , \\ A = 0.2531 \quad , \quad B = 0.2117 \quad , \quad (w = 0.01 \text{ m} \quad , \quad h = 0.02 \text{ m}) \quad , \end{aligned} \quad (5.5)$$

It is expected on the basis of Eq. (4.26) that A and B should be close to one for $w/h \geq 2$.

The small discrepancy between the accurate and approximate curves of Fig. 2 is due mainly to the slightly rough treatment of exponential terms in the latter; for instance, the use of approximation Eq. (2.18) for Eq. (2.17).

To check our results at the highest frequency, we use the computer code of Ref. 2. The code is based on the Olver expansions which are valid in Regions 2 and 3. In the $p = 1$ mode, which is dominant, the accurate curve of Fig. 2 agrees to four digits with the Olver code at $\nu = (R/h)^{1/2} = 16.88$

Similar results were obtained for a variety of geometrical parameters R, a, b and h .

ACKNOWLEDGMENTS

We thank Alessandro Ruggiero and Joseph Bisognano for encouraging us to make this study.

APPENDIX A.

COMPARISON AND TESTS OF ASYMPTOTIC EXPANSIONS

Here we show that the Debye expansions carried to second order yield good approximations to the relevant Bessel functions throughout Regions 1 and 2. First, we consider the large-argument expansion,

$$I_n(x) \sim \left(\frac{1}{2\pi x}\right)^{1/2} e^x [1 - a_1 + a_2 - a_3 + \dots] \quad (A1)$$

where

$$a_1 = \frac{\mu - 1}{8x}, \quad a_2 = \frac{(\mu - 1)(\mu - 9)}{2!(8x)^2}, \quad a_3 = \frac{(\mu - 1)(\mu - 9)(\mu - 25)}{3!(8x)^3}, \quad (A2)$$

$$\mu = 4n^2.$$

At large ν the highest power of μ in the coefficients Eq. (A2) is dominant. To ensure that the first few coefficients a_k fall off rapidly with increasing k , we must therefore require, with $x = \Gamma_p R$, that

$$\frac{\mu}{8x} = \frac{\nu^2}{2\beta^2} \frac{R}{h} \frac{1}{[(\pi p)^2 - \nu^2]^{1/2}} \ll 1. \quad (A3)$$

If β is not small compared to one, Eq. (A3) will be achieved if ν lies in Region 1,

$$0 < \nu < \left(\frac{h}{R}\right)^{1/2}. \quad (A4)$$

Here we have regarded $1/2\pi$ as adequately small compared to one, which will be justified presently by numerical tests.

Table 1 compares the Debye and large argument expansions of $I_n(\Gamma_p R)$, showing the ratio

$$\frac{I_n(\Gamma_p R) \text{ (Debye)}}{I_n(\Gamma_p R) \text{ (large-argument)}} = 1 + \epsilon_I, \quad (A5)$$

expressed in terms of the discrepancy ϵ_I for frequencies ranging over Region 1. For each expansion, we take terms up to fourth order, tabulating the coefficients a_k of Eq. (A1) and c_k of Eq. (3.5). The calculation was done in double precision; i.e., to 15 or 16 digits accuracy. The terms c_i of the Debye series are nearly constant over Region 1 because of the large values of z_R . Throughout Region 1, the Debye series behaves just as the large-argument series behaves at $\nu = 0$, which is to say that

the terms drop off very rapidly. At the upper end of Region 1, the terms of the large-argument series fall off slowly, as was expected from our argument concerning Eq. (A3). The small values of the discrepancy ϵ_I indicate that either series can be used successfully in Region 1.

One can verify that the Debye expansion for $I_n(nz)$, with fixed $nz = x$, goes over into the large-argument expansion, Eq. (A1), as $n \rightarrow 0$. Moreover, one can make Taylor expansions in ν and identify coefficients of a few terms to see that the two expansions should agree at small but nonzero ν . This is an interesting property of the Debye expansion which may have wider applications. We are not aware of the result being generally known.

In Region 2a, defined in Eq. (3.3), the Debye expansion will work even better than in Region 1, since n is larger and the approximation to $I_n(nz)$ is uniform in z . In Region 2b, n is bigger yet and the approximation to $J_n(ny)$ remains good until we approach the singularity of the coefficients at $y = 1$. The highest powers of t in the coefficients c_k of Eq. (3.13) dominate. The requirement for fixing the upper limit of Region 2b, analogous to Eq. (A3), is

$$\frac{t^3}{n} \ll 1. \quad (\text{A6})$$

To evaluate $t = (1 - y^2)^{-1/2}$, recall that

$$y = \frac{\gamma p r}{n} = \beta \left[1 - \left(\frac{\pi p}{\nu} \right)^2 \right]^{1/2} \frac{r}{R}, \quad (\text{A7})$$

and let $r = R + x/2$, $|x| < 2w$. Since $(x/R)^2 \ll 1$, we see that

$$\begin{aligned} 1 - y^2 &\approx \left(\frac{\pi p \beta}{\nu} \right)^2 \left(1 + \frac{x}{R} \right) - \beta^2 \frac{x}{R} + \frac{1}{\gamma^2} \\ &= \left(\frac{\pi p \beta}{\nu} \right)^2 + \frac{1}{\gamma^2} + \mathcal{O}\left(\frac{x}{R}\right). \end{aligned} \quad (\text{A8})$$

Hence, for a rough value at $\beta \approx 1$,

$$\frac{t^3}{n} \approx \left(\frac{\nu}{\pi p} \right)^3 \frac{h}{\nu R}, \quad (\text{A9})$$

and Eq. (A6) is satisfied for $\nu < (R/h)^{1/2}$.

Now let us assess accuracy of the Debye expansion carried to second order by comparing to the same carried to higher order. We make the comparison for the particular combinations of Bessel functions that occur in the impedance; namely, Eqs. (3.21) and (3.23). As an accurate standard, we take Eq. (3.21) carried to fourth order and Eq. (3.23) computed with each of its four component series taken to fourth order. For Eq. (3.23) we do not invert the denominators by Taylor expansion, just taking the formula as it stands. We then compare these accurate evaluations to Eq. (3.21) taken to second order and to Eq. (3.24), respectively. With the same choice of parameters and frequencies as in Table 1, we compute

$$\frac{I_n(\Gamma_p R) K_n(\Gamma_p R) [\text{Eq.}(3.21), \text{second order}]}{I_n(\Gamma_p R) K_n(\Gamma_p R) [\text{standard}]} = 1 + \epsilon_{IK}, \quad (\text{A10})$$

$$\frac{R_{np}^{(M)}(b, R) [\text{Eq.}(3.24)]}{R_{np}^{(M)}(b, R) [\text{standard}]} = 1 + \epsilon_R. \quad (\text{A11})$$

We find $\epsilon_{IK} = -3.2 \cdot 10^{-13}$, and $\epsilon_R = -9.4 \cdot 10^{-13}$, these values being almost constant over Region 1. We conclude that the second order Debye expansion is extremely accurate in Region 1. It will be even better in Region 2a and a large part of Region 2b. To assess accuracy at the upper end of Region 2b, one can make comparisons with the Olver expansions, which are valid throughout Regions 2 and 3. The computer code written in connection with Ref. 2 is used in Sec. 5 to make such a comparison. The result is that the second order formulas are still quite good at the top of Region 2b.

The errors quoted above were for R/h typical of a fairly small ring. For yet smaller R/h , the errors will be larger but still negligible, even for very small rings like the “compact light sources” now being built.

APPENDIX B. ESTIMATE OF THE EXPONENTIAL TERM Ψ

To estimate Ψ as defined in Eq. (4.15), we first examine its leading approximation Ψ_o as defined in Eq. (4.20). We denote exponential factors as follows:

$$E_{bR} = \exp\{-2\pi p \mu_p (b - R)/h\}. \quad (B1)$$

Using Eqs. (4.1), (4.4), and (4.7), we can easily evaluate Ψ_o at $\nu = 0$ and $\nu = \pi p$:

$$\Psi_o = \begin{cases} -\frac{\beta^2}{2} \left(\frac{h}{\pi p R}\right)^2 \left[E_{bR} \frac{b-R}{b} + E_{Ra} \frac{R-a}{a} \right], & \nu = 0, \\ \frac{\beta^4}{2} \left(\frac{h}{\pi p R}\right)^2 \left[E_{bR} \frac{b^2 - R^2}{R^2} + E_{Ra} \frac{R^2 - a^2}{R^2} \right], & \nu = \pi p. \end{cases} \quad (B2)$$

To illustrate let us take a centered beam and compare Ψ_o to the curvature part of Φ , the second term in Eq. (4.13), for $w = h$ and $w = 2h$ with $\beta = 1$. The values at $\nu = 0$ and πp are both the same:

$$\frac{\Psi_o}{\Phi^{\text{curv.}}} \Big|_{\nu=0, \pi p} = \begin{cases} -2\pi p e^{-\pi p}, & w = h, \\ -4\pi p e^{-2\pi p}, & w = 2h, \end{cases} = \begin{cases} -(0.27, .0015), & p = (1, 3), \\ -(0.023, 2.4 \times 10^{-7}), & p = (1, 3). \end{cases} \quad (B3)$$

Thus, Ψ gives an appreciable contribution only when the aspect ratio w/h is small and, in any case, only for $p = 1$. The same conclusion holds throughout the interval $0 < \nu < \pi p$, as one can see by making a simple upper bound of Eq. (4.20). Since t_r decreases with increasing r in this region,

$$\frac{t_b^2 t_R}{t_b + t_R} < \frac{t_R^3}{2t_b} < \frac{b t_R^2}{R 2}, \quad \frac{t_R^2 t_a}{t_a + t_R} < \frac{t_R t_a}{2} < \frac{R t_R^2}{a 2}. \quad (B4)$$

Also, $|1 - t_b^2 - t_b t_R - t_R^2| \leq 2$ and

$$\frac{1}{\nu^2} = \frac{z^2 + \beta^2}{(\beta \pi p)^2} < \frac{1}{(t_R \beta \pi p)^2}, \quad (B5)$$

so that an upper bound is

$$|\Psi_o| < \frac{1}{2} \left(\frac{\beta h}{\pi p R}\right)^2 \left[E_{bR} \frac{b}{R} \frac{b^2 - R^2}{R^2} + E_{Ra} \frac{R}{a} \frac{R^2 - a^2}{a^2} \right], \quad (B6)$$

$$0 < \nu < \pi p.$$

To make an upper bound in Region 2b, where $\pi p < \nu < (R/h)^{1/2}$, we must account for the fact that all of the z_r^2 are negative and increase in magnitude with increasing r . Thus, $t_r > 1$ is an increasing function of r and $|1 - t_b^2 - t_b t_R - t_R^2| < 3t_b^2$, so that

$$|\Psi_o| < \frac{3}{4} \left(\frac{\beta h}{\pi p R} \right)^2 \left[E_{bR} \frac{t_b^4}{t_R^2} \frac{b^2 - R^2}{R^2} + E_{Ra} t_b^2 \frac{R^2 - a^2}{a^2} \right]. \quad (B7)$$

Furthermore,

$$\begin{aligned} 1 + z_b^2 > \beta^2 + z_b^2 &= \beta^2 \left\{ 1 + \left(\frac{b}{R} \right)^2 \left[\left(\frac{\pi p}{\nu} \right)^2 - 1 \right] \right\}, \\ &= \left(\frac{\beta \pi p}{\nu} \right)^2 \left\{ \left(\frac{b}{R} \right)^2 - \left(\frac{\nu}{\pi p} \right)^2 \frac{x}{R} \left(1 + \frac{x}{4R} \right) \right\}, \end{aligned} \quad (B8)$$

where $b = R + x/2$, $|x| < 2w$. Recalling that $\nu^2 < R/h$, we assume that

$$\pi^2 h > x \left(1 + \frac{x}{4R} \right), \quad (B9)$$

as will usually be the case, so that $\beta^2 + z_b^2 > 0$. It follows from our upper limit on ν that

$$t_b^2 \leq \left(\frac{\nu}{\beta \pi p} \right)^2 I^{-1}, \quad (B10)$$

$$I = \left(\frac{b}{R} \right)^2 - \frac{1}{(\pi p)^2} \frac{x}{h} \left(1 + \frac{x}{4R} \right). \quad (B11)$$

The constant I is close to one unless the aspect ratio w/h is unusually large. Since

$$1 + z^2 = \frac{1}{\gamma^2} + \left(\frac{\beta \pi p}{\nu} \right)^2, \quad (B12)$$

we have, from Eqs. (B7), (B10), and (B12),

$$|\Psi_o| < \frac{3}{4} \left(\frac{\nu}{\pi p} \right)^2 \left(\frac{h}{\pi p R} \right)^2 \left[E_{bR} \frac{1 + (\nu/\beta\gamma\pi p)^2}{I^2} \frac{b^2 - R^2}{R^2} + E_{Ra} \frac{R^2 - a^2}{R^2} \right]. \quad (B13)$$

At $\beta = 1$ the main difference between Eq. (B13) and the low frequency bound Eq. (B6) is a factor

$$\frac{3}{2} \left(\frac{\nu}{\pi p} \right)^2 \leq \frac{3}{2} \frac{R}{h} \frac{1}{(\pi p)^2}. \quad (B14)$$

But notice that Φ in Eq. (4.13) also has a term with factor $(\nu/\pi p)^2$, so that the ratio Ψ_o/Φ retains roughly the same bound over our entire frequency range. At the highest frequency, the parameter h/R — rather than $(h/R)^2$ — sets the overall scale of the impedance.

Having shown that there is no close cancellation between Ψ_o and Φ (the former being much smaller than the latter in most cases), we can now show that Ψ_o is a good approximation to Ψ , as defined in Eq. (4.15). We only have to show that $2d_2 - d_1^2$ and $\epsilon(b, R)$, $\epsilon(R, a)$ of Eqs. (4.15) and (4.16) are small compared to one. By Eqs. (4.2) and (4.6) we obtain

$$|2d_2 - d_1^2| < \frac{|z^2(-3z^2 + 4)|}{8(1 + z^2)^2} \left(\frac{h}{\pi p R} \right)^2. \quad (B15)$$

For $\nu < \pi p$ we have $0 < z < \infty$. Finding the maximum over z of the function (B.15), we obtain

$$|2d_2 - d_1^2| < \frac{1}{14} \left(\frac{h}{\pi p R} \right)^2, \quad \nu < \pi p. \quad (B16)$$

On the other hand, in Region 2b we have $|z^2| < \beta^2$ and Eq. (B12) so that

$$|2d_2 - d_1^2| < \frac{7}{8} \frac{\nu^4}{\beta^2} \left(\frac{h}{R} \right)^2 \frac{1}{(\pi p)^6} < \frac{1}{\beta^2} \frac{1}{(\pi p)^6}, \quad (B17)$$

$$\pi p < \nu < \left(\frac{R}{h} \right)^{1/2}.$$

We can therefore neglect $2d_2 - d_1^2$ in comparison to one, but at the highest frequencies this quantity is small only by virtue of inverse powers of πp , not because of geometrical factors like $(h/R)^2$. Here we are seeing the expected slow fall-off of Debye series terms at the upper end of Region 2b.

To bound $\epsilon(b, R)$, $\epsilon(R, a)$, we use the same sort of arguments that we used to bound Ψ_o . For $0 < \nu < \pi p$,

$$|\epsilon(b, R)| = \frac{1}{12\pi p} \frac{h}{R} (z^2 + \beta^2)^{1/2} z^2 \frac{(t_R t_b)^2}{t_R + t_b} \frac{b^2 - R^2}{R^2} \quad (B18)$$

$$\times |-3 + t_b^2 + t_b t_R + t_R^2| < \frac{1}{8\pi p} \frac{h}{R} \frac{b^2 - R^2}{R^2}.$$

For $\pi p < \nu < (R/h)^{1/2}$,

$$\begin{aligned}
 |\epsilon(b, R)| &< \frac{1}{8\pi p} \frac{h}{R} (z^2 + \beta^2)^{1/2} |z^2| t_b^4 t_R \frac{b^2 - R^2}{R^2} , \\
 &< \frac{1}{8\pi p} \frac{h}{R} \beta^2 t_b^4 \frac{b^2 - R^2}{R^2} < \frac{1}{8\pi p} \frac{h}{R} \frac{b^2 - R^2}{R^2} \left(\frac{\nu}{\pi p} \right)^4 \frac{1}{(\beta I)^2} ,
 \end{aligned} \tag{B19}$$

where $I \approx 1$ is defined in Eq. (B11). The pattern is the same as before: $\epsilon(b, R)$ is small by virtue of a factor $[(b - R)h]/R^2$ at low frequency, but only by a factor $(1/4)(\pi p)^{-5}$ at the highest frequency. Similar bounds hold for $\epsilon(R, a)$; consequently, both ϵ terms may be dropped.

APPENDIX C. ESTIMATE OF EXPONENTS

Here we wish to estimate the exponents that arise from the Debye expansions of Bessel functions, as carried out in Sec. 4. We study the quantity

$$n [\eta(z_b) - \eta(z_R)] , \quad (C1)$$

where

$$\eta(z) = (1 + z^2)^{1/2} + \ln \frac{|z|}{1 + (1 + z^2)^{1/2}} ,$$

$$z_r^2 = \left(\beta \frac{r}{R} \right)^2 \left[\left(\frac{\pi p}{\nu} \right)^2 - 1 \right] , \quad (C2)$$

$$n = \frac{\pi p R}{h} \frac{1}{(\beta^2 + z_R^2)^{1/2}} .$$

For estimating differences, one can use the mean-value theorem in the form

$$f(r_2) - f(r_1) = f'(r_1) (r_2 - r_1) + \Phi(r_1, r_2) ,$$

$$|\Phi(r_1, r_2)| \leq \frac{1}{2} (r_2 - r_1)^2 \max_{r_1 \leq u \leq r_2} |f''(u)| , \quad (C3)$$

which holds for any function with a continuous second derivative on $[r_1, r_2]$.

First, consider the case $0 < \nu < \pi p$ (Regions 1 and 2a), or $0 < z_r < \infty$. To estimate Eq. (C1) note that

$$\eta'(z) = \frac{(1 + z^2)^{1/2}}{z} . \quad (C4)$$

Apply (C3) with $f(r) = \eta(z_r)$, $r_1 = R$, $r_2 = b$. We have

$$f'(r) = \eta'(z_r) \frac{dz_r}{dr} = \frac{(1 + z_r^2)^{1/2}}{r} ,$$

$$f''(r) = -\frac{1}{r^2(1 + z_r^2)^{1/2}} . \quad (C5)$$

Now

$$n [\eta(z_b) - \eta(z_R)] = n [f(b) - f(R)] ,$$

$$= n f'(R)(b - R) + n \Phi(R, b) , \quad (C6)$$

where

$$\begin{aligned}
n f'(R)(b-R) &= \left[\pi p \frac{R}{h} \frac{1}{(\beta^2 + z_R^2)^{1/2}} \right] \frac{(1 + z_R^2)^{1/2}}{R} (b-R) \\
&= \pi p \frac{b-R}{h} \left[1 + \frac{1}{\gamma^2(\beta^2 + z_R^2)} \right]^{1/2} = \pi p \mu_p \frac{b-R}{h},
\end{aligned} \tag{C7}$$

the function μ_p being as defined in Eq. (4.19) and

$$\begin{aligned}
|n\Phi(R, b)| &\leq \pi p \frac{R}{h} \frac{1}{(\beta^2 + z_R^2)^{1/2}} \frac{1}{2} (b-R)^2 \max_{R \leq r \leq b} |f''(r)|, \\
&= \frac{\pi p R}{2h} \frac{(b-R)^2}{R^2} \frac{1}{(\beta^2 + z_R^2)^{1/2}} \frac{1}{(1 + z_R^2)^{1/2}} \leq \frac{\pi p}{2\beta} \frac{(b-R)^2}{hR}.
\end{aligned} \tag{C8}$$

Thus, for $0 < \nu < \pi p$,

$$n[\eta(z_b) - \eta(z_R)] = \pi p \mu_p \frac{b-R}{h} + \epsilon, \tag{C9}$$

where the remainder ϵ is smaller than the main term by at least a factor

$$\frac{1}{2\beta} \frac{b-R}{R}, \tag{C10}$$

which is $w/4\beta R$ for a centered beam.

For $\pi p < \nu < (R/h)^{1/2}$ (Region 2b), let $y = |z|$ and regard η as a function of y :

$$\eta(y) = (1 - y^2)^{1/2} + \ln \frac{y}{1 + (1 - y^2)^{1/2}}. \tag{C11}$$

The function of interest is

$$n[\eta(y_b) - \eta(y_R)],$$

where

$$y_r^2 = \left(\beta \frac{r}{R} \right)^2 \left[1 - \left(\frac{\pi p}{\nu} \right)^2 \right] = -z_r^2. \tag{C12}$$

The derivative of η is

$$\eta'(y) = \frac{(1 - y^2)^{1/2}}{y}. \tag{C13}$$

With $f(r) = \eta(y_r)$, the computation of the leading term in the mean value theorem is the same as before, but the bound on the remainder is different: instead of Eq. (C8) we have

$$\begin{aligned}
|n\Phi(R, b)| &\leq \frac{\pi p}{2} \frac{(b-R)^2}{Rh} \frac{1}{(\beta^2 - y_R^2)^{1/2}} \max_{R \leq r \leq b} \frac{1}{(1 - y_r^2)^{1/2}} \\
&< \frac{\pi p}{2} \frac{(b-R)^2}{Rh} \frac{1}{(\beta^2 - y_R^2)^{1/2}} \frac{1}{(\beta^2 - y_b^2)^{1/2}} .
\end{aligned} \tag{C14}$$

But with $b = R + x/2$ we have as in Eqs. (B8) and (B11),

$$\begin{aligned}
\beta^2 - y_b^2 &= \beta^2 \left[-\frac{x}{R} \left(1 + \frac{x}{4R}\right) + \left(\frac{b \pi p}{R \nu}\right)^2 \right] , \\
&\geq \left(\frac{\beta \pi p}{\nu}\right)^2 I
\end{aligned} \tag{C15}$$

and

$$\beta^2 - y_b^2 = \left(\frac{\beta \pi p}{\nu}\right)^2 \geq (\beta \pi p)^2 \frac{h}{R} . \tag{C16}$$

Again we assume the condition (B9). Now Eq. (C14) gives

$$|n\Phi(R, b)| < \frac{1}{2(\beta \pi p)^2} \left(\frac{b-R}{h}\right)^2 I^{-1/2} . \tag{C17}$$

The final factor $I^{-1/2}$ is close to one unless the aspect ratio w/h is unusually large. Thus at our highest frequency, the error ϵ in (C.9) is less than the main term by at least a factor

$$\frac{1}{2\beta^2(\pi p)^3} \frac{b-R}{h} . \tag{C18}$$

Although this lacks the small geometrical factor of Eq. (C10), it is still typically small compared to one. The error becomes large in Region 3. published in Particle Accelerators.

REFERENCES

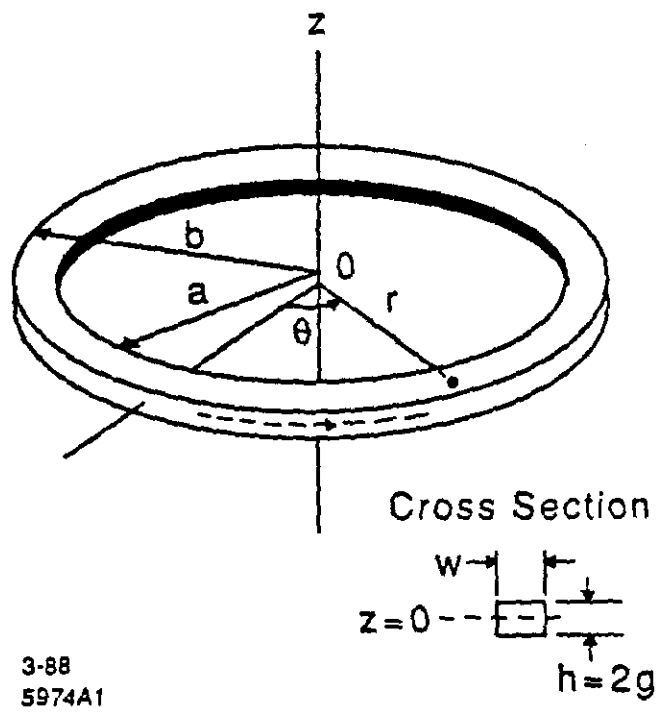
1. King-Yuen Ng, SSC-Fermilab report SSC-163/FN-477, to be
2. R. L. Warnock and P. Morton, SLAC-PUB-4562, to be published in Particle Accelerators.
3. A. Ruggiero, private communication.
4. M. Zisman, Lawrence Berkeley Laboratory Report LBL-25335.
5. V. K. Neil, "A Study of Some Coherent Electromagnetic Effects in High-Current Particle Accelerators," Ph.D. Thesis, University of California, Berkeley, 1960.
6. M. Abramowitz and I. A. Stegun, eds., *Handbook of Mathematical Functions* (Dover, New York, 1965). We refer to formula numbers of this text as A.-S. 9.7.1, etc.

Table I

ν	ϵ_I	$-a_1$ c_1	a_2 c_2	$-a_3$ c_3	a_4 c_4
0	$< 10^{-16}$	1.396×10^{-4} 1.396×10^{-4}	8.771×10^{-8} 8.771×10^{-8}	1.020×10^{-10} 1.020×10^{-10}	1.745×10^{-13} 1.745×10^{-13}
1.185×10^{-2}	7.2×10^{-16}	-6.226×10^{-3} 1.396×10^{-4}	1.591×10^{-5} 8.770×10^{-8}	-1.525×10^{-8} 1.020×10^{-10}	-1.810×10^{-12} 1.745×10^{-13}
2.369×10^{-2}	3.0×10^{-11}	-2.532×10^{-2} 1.396×10^{-4}	3.065×10^{-4} 8.768×10^{-8}	-2.245×10^{-6} 1.020×10^{-10}	1.045×10^{-8} 1.743×10^{-13}
3.554×10^{-2}	3.5×10^{-9}	-5.716×10^{-2} 1.396×10^{-4}	1.602×10^{-3} 8.764×10^{-8}	-2.872×10^{-5} 1.019×10^{-10}	3.623×10^{-7} 1.740×10^{-13}
4.739×10^{-2}	7.9×10^{-8}	-1.017×10^{-1} 1.396×10^{-4}	5.117×10^{-3} 8.759×10^{-8}	-1.678×10^{-4} 1.018×10^{-10}	3.987×10^{-6} 1.737×10^{-13}
5.923×10^{-2}	8.4×10^{-7}	-1.590×10^{-1} 1.395×10^{-4}	1.256×10^{-2} 8.753×10^{-8}	-6.517×10^{-4} 1.016×10^{-10}	2.482×10^{-5} 1.732×10^{-13}

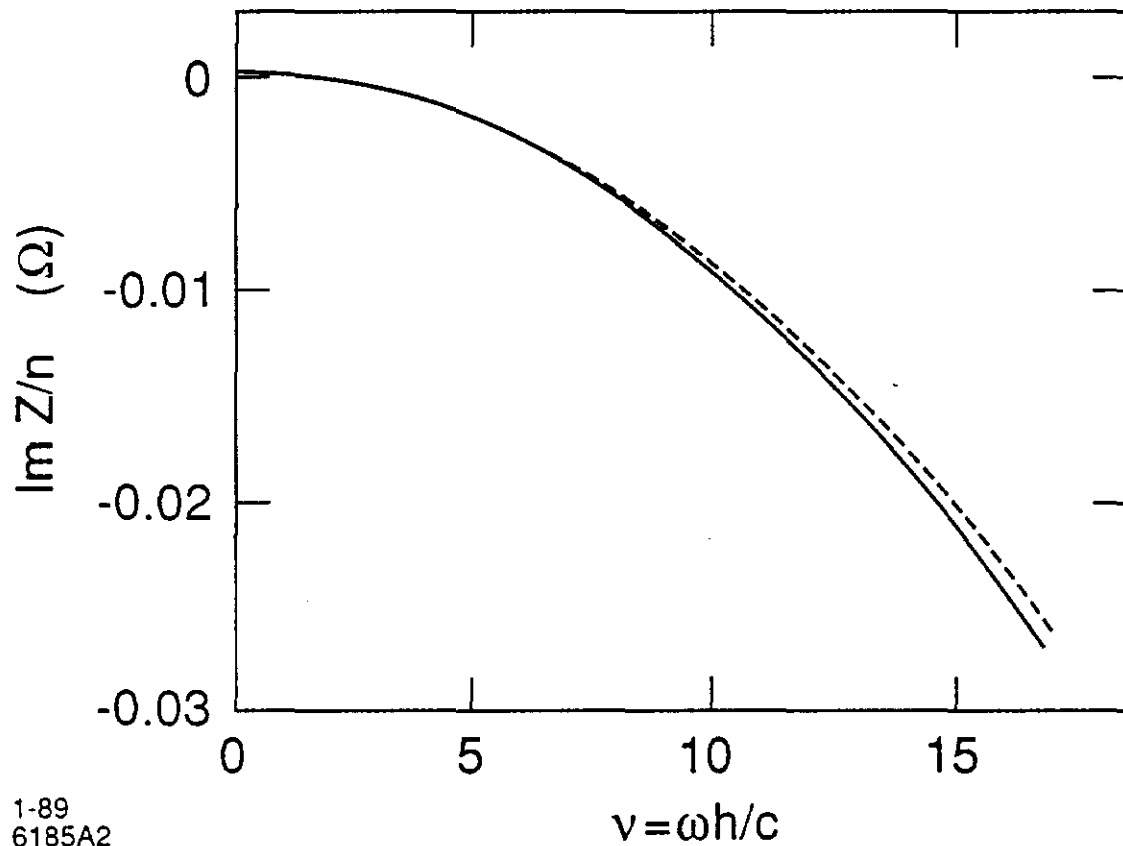
FIGURE CAPTIONS

- Fig. 1. Smooth toroidal chamber with rectangular cross section.
- Fig. 2. Reactive impedance of the smooth toroidal chamber, plotted as $Im Z(n, n\omega_0)/n$ vs. $\nu = \omega h/c$, for $\beta = 1$. The reactive impedance is positive at zero frequency, first turning negative near $\nu = \pi/\sqrt{3}$. This zero is typically in the neighborhood of the lowest TE cutoff, as given by Eq. (1.3). The solid curve is the accurate value from Eq. (2.19) and fourth-order Debye expansions. The dashed curve is the approximate value from Eq. (4.23). Parameters: $R = 5.7$ m, $w = h = 2$ cm, $\beta = 1$.



3-88
5974A1

Fig. 1



1-89
6185A2

Fig. 2